

Original Manuscript

Genotoxicity of TiO₂ nanoparticles assessed by mini-gel comet assay and micronucleus scoring with flow cytometry

Sebastiano Di Bucchianico¹, Francesca Cappellini¹, Florane Le Bihanic¹, Yuning Zhang^{1,2}, Kristian Dreij¹ and Hanna L. Karlsson^{1,*}

¹Institute of Environmental Medicine, Karolinska Institutet, Nobels väg 13, 171 77 Stockholm, Sweden and ²Department of Fibre and Polymer Technology, KTH Royal Institute of Technology, School of Chemical Science and Engineering, Teknikringen 42, 100 44 Stockholm, Sweden

*To whom correspondence should be addressed. Tel: +46 8 524 800 00; Fax: + 46 8 33 69 81; Email: Hanna.L.Karlsson@ki.se

Received 8 April 2016; Revised 3 June 2016; Accepted 6 June 2016.

Abstract

The widespread production and use of nanoparticles calls for faster and more reliable methods to assess their safety. The main aim of this study was to investigate the genotoxicity of three reference TiO₂ nanomaterials (NM) within the frame of the FP7-NANoREG project, with a particular focus on testing the applicability of mini-gel comet assay and micronucleus (MN) scoring by flow cytometry. BEAS-2B cells cultured under serum-free conditions were exposed to NM100 (anatase, 50–150 nm), NM101 (anatase, 5–8 nm) and NM103 (rutile, 20–28 nm) for 3, 24 or 48 h mainly at concentrations 1–30 µg/ml. In the mini-gel comet assay (eight gels per slide), we included analysis of (i) DNA strand breaks, (ii) oxidised bases (Fpg-sensitive sites) and (iii) light-induced DNA damage due to photocatalytic activity. Furthermore, MN assays were used and we compared the results of more high-throughput MN scoring with flow cytometry to that of cytokinesis-block MN cytome assay scored manually using a microscope. Various methods were used to assess cytotoxic effects and the results showed in general no or low effects at the doses tested. A weak genotoxic effect of the tested TiO₂ materials was observed with an induction of oxidised bases for all three materials of which NM100 was the most potent. When the comet slides were briefly exposed to lab light, a clear induction of DNA strand breaks was observed for the anatase materials, but not for the rutile. This highlights the risk of false positives when testing photocatalytically active materials if light is not properly avoided. A slight increase in MN formation for NM103 was observed in the different MN assays at the lower doses tested (1 and 5 µg/ml). We conclude that mini-gel comet assay and MN scoring using flow cytometry successfully can be used to efficiently study cytotoxic and genotoxic properties of nanoparticles.

Introduction

The widespread production and use of nanoparticles (NPs) in many industrial and biomedical applications calls for faster and more reliable methods to assess their safety. Critical effects include DNA damage and interference with the mitotic machinery. Such effects can result in pre-mutagenic lesions and chromosome instability possibly leading to mutations and cancer as well as to other adverse outcomes. The comet

assay and micronucleus (MN) test are the two most commonly used genotoxicity tests assessing NP-induced damage at DNA and chromosome level, respectively. However, in their original version, both assays are rather labour intensive and time consuming, thus calling for the need of testing more high-throughput variants (1). Furthermore, both assays have shown different concerns regarding possible false-positive or false-negative results depending on NP–assay interactions (2,3). The main concern for the interactions within the comet assay is that

NPs have been observed in the 'head' of the comets during scoring (4), suggesting that these NPs were present during the assay performance. In principal, such NPs may, e.g., induce additional breaks in 'naked DNA' during the assay or may affect the migration of DNA under electrophoresis (3,5). Furthermore, oxidative stress caused by NPs may be underestimated if the NPs, or released ions, affect the Fpg (formamidopyrimidine-DNA glycosylase) enzyme used to detect oxidative DNA damage (6). For most NPs, however, an interaction that significantly impacts the comet assay results is unlikely (3,7). For the MN assay, interaction due to cytochalasin-B treatment has been described (7). Cytochalasin-B is used to identify the nuclei that have undergone one division during the exposure, but the treatment can also decrease cellular uptake of the NPs as a consequence of actin inhibition (2). Another limitation of the method is the difficulties to score the slides in the case of high NP exposure concentrations leading to high deposition of NPs on the cells (8).

Collectively, this knowledge suggests putting a certain effort in developing more reliable and faster testing strategies compared to the existing ones, suitable for a high number of nanomaterials (NM). A good starting point is to carefully assess the methodology used to disperse NPs. In the present study, performed within the frame of the European project NANoREG (www.nanoreg.eu), a probe sonicator calibration standard operating procedure was developed in order to generate both intra- and inter-laboratory reproducible dispersions when using a standardised dispersion protocol (NANOGENOTOX). One important aim of the NANoREG project is 'testing the tests', meaning testing the most frequently used assays for various endpoints for commonly used NM. One of the NM produced in high volume today is titanium dioxide (TiO₂) NP, used in various consumer products including sunscreens (9). Titanium dioxide (not specifically in nano form) has been classified as a Group 2B carcinogen (possibly carcinogenic to humans) by IARC, and genotoxicity studies show in general mixed results with both positive and negative outcomes. We recently reviewed *in vitro* genotoxicity studies of NPs using both comet assay and MN assay and found in general a good consistency between the methods, but a poorer correlation in the case of TiO₂. Furthermore, a brief light exposure of comet slides with cells treated with TiO₂ NPs substantially increased the DNA strand breaks for photocatalytically active NPs (3). Taken together, it is difficult to draw an overall conclusion from existing genotoxicity studies of TiO₂ depending in part of methodological considerations and lack of NP characterisation.

The main aim of this study was to investigate the genotoxicity of three reference TiO₂ materials obtained from the Joint Research Center (Ispra, Italy); NM100, NM101 and NM103 dispersed according to standard procedures, with a particular focus on testing the applicability of mini-gel comet assay and MN scoring by flow cytometry. We used human bronchial epithelial BEAS-2B cells cultured under serum-free conditions since serum proteins can affect the genotoxicity of NPs (10,11). To test more time-efficient methods, we used mini-gel comet assay (eight gels per slide) and included analysis of (i) single and double DNA strand breaks, (ii) oxidised bases by using the Fpg enzyme and (iii) light-induced DNA damage due to photocatalytic activity of TiO₂ NPs. Furthermore, MN assays were used and we investigated the applicability of more high-throughput MN scoring with flow cytometry and compared the results to the cytokinesis-block MN cytome (CBMN Cyt) assay scored manually using a microscope.

Materials and methods

Preparation of particle dispersions

TiO₂ NM100 (anatase, 50–150 nm, Brunauer–Emmett–Teller (BET) area 9.2 m²/g), NM101 (anatase, 5–8 nm, BET area 316 m²/g) and

NM103 (rutile, 20–28 nm, BET area 51 m²/g) were obtained from the repository of the European Commission Joint Research Centre, Institute for Health and Consumer Protection (JRC-IHCP; Ispra, Italy). Their crystalline phase, crystallite size, specific surface area and other physico-chemical properties are available in the JRC report (12). In this report, NM100 is reported to be non-coated, whereas NM101 and NM103 are coated. Particle powders were suspended in 0.05% bovine serum albumin (BSA) at a concentration of 2.56 mg/ml and were then sonicated for 15 min and 30 s using a MSE Soniprep 150 equipped with an exponential microprobe (Microtip type 38121-114A) at 22 micron amplitude in a continuous mode. This setup resulted in an average power of 7.56 (±0.01) W and a sample specific energy of 7056 J according to calibrations performed in the frame of NANoREG project. During sonication, the samples were cooled in icy water to prevent excessive heating. After sonication, stock suspensions were prepared by diluting the samples in 0.05% BSA to reach a final concentration of 0.1 mg/ml. Aliquots of the stock suspensions were diluted in culture medium to obtain the desired test concentrations.

Dynamic light scattering

Dynamic light scattering (DLS) measurements were performed with a Malvern Zetasizer Nano TZ equipped with a 633-nm laser diode operating at an angle of 173°. One millilitre of well-dispersed sample (1 and 15 µg/ml of TiO₂ NPs in culture medium) was transferred into a DLS cuvette of clear disposable for size distribution analysis and folded capillary zeta cells for zeta potential measurement. Samples were allowed to equilibrate for 120 s before each measurement, and 10 repeated measurements were performed for each sample at 37°C. Cumulants analysis (auto-setting by instrument) was used in order to obtain intensity size distribution.

Cells and cell culture conditions

The immortalised human bronchial epithelial cell lines (BEAS-2B, European Collection of Cell Cultures) were cultured in bronchial epithelial cell growth medium (BEGM; Lonza) supplemented with human epidermal growth factors (hydrocortisone, insulin, bovine pituitary extract, gentamicin and amphotericin-B, transferrin, triiodothyronine, retinoic acid and epinephrine) according to manufacturer's instructions (BEGM SingleQuots Kit, Lonza). The cells were seeded in flasks or multi-well plates pre-coated with a mixture of 0.01 mg/ml fibronectin, 0.03 mg/ml bovine collagen type I, 0.01 mg/ml BSA and 0.2% penicillin–streptomycin in BEGM supplement-free medium. The cells were incubated in a humidified atmosphere at 37°C, 5% CO₂ and subcultured at 80% confluency for no more than 10 passages. For each experiment, BEAS-2B cells were seeded one day prior to particles exposures, at an approximate density of 6 × 10⁴ cells/cm² for 24- and 48-h exposure and 15 × 10⁴ cells/cm² for 3-h exposure in indicated cell culture plates. The final exposure volumes used in different plates were determined in order to keep the same µg/cm² correspondence between exposures in different plates.

Cell viability

The Alamar Blue reagent, a water-soluble resazurin dye, was used to evaluate cell viability as a function of resazurin reduction to red fluorescent dye resofurin by metabolically active cells. BEAS-2B cells were seeded in transparent 96-well plates and exposed to NM100, NM101 or NM103 TiO₂ dispersions at mass concentrations ranging from 2 to 100 µg/ml (0.62–31.25 µg/cm²) for 3, 24 or 48 h. After exposure, cells were washed and a 10% Alamar Blue solution (ThermoFisher Scientific) was added in each well and incubated for

2 h at 37°C. Blank control wells without cells were prepared for each particle dispersion to exclude possible interactions with the assay. In these control wells, the Alamar Blue reagent was directly added to reach a 10% final concentration. Cells treated with 0.1% Triton X-100 (Sigma–Aldrich) was used as a positive control. The fluorescence was measured on a VICTOR³ V multilabel reader (PerkinElmer) with an excitation wavelength of 560 nm and an emission wavelength of 590 nm. The fluorescence values were normalised by the controls and expressed as percent viability.

CBMN Cyt assay

Cytotoxicity, cytostasis and chromosomal damage were studied by CBMN Cyt assay. BEAS-2B cells were seeded in six well plates and exposed to NM100, NM101 or NM103 TiO₂ dispersions at 1, 5 or 15 µg/ml (0.2–3.2 µg/cm²) for 48 h. About 0.05 µg/ml mitomycin-C was used as a positive control. A delayed co-treatment with cytochalasin-B was used. Following 20-h exposures, 5 µg/ml cytochalasin-B (Sigma–Aldrich) was used to block cytokinesis, and cells were harvested after additional 28 h, then treated 1 min with 0.04 M KCl (hypotonic solution), washed twice with fresh cold fixative (methanol:acetic acid 6:1) and placed at –20°C overnight. Finally, cell solutions were loaded onto clean and cold glass slides. The air-dried slides were stained with 2% (v/v) Giemsa solution (Sigma–Aldrich) in deionised water for 20 min. As described by Fenech (13), Di Bucchianico *et al.* (14) and the OECD guideline 487 (15), 1000 cells were scored to evaluate cytostasis as a reduction of replication index of the treated cells compared to the negative control. The number of apoptotic, necrotic and mitotic cells per 1000 cells was also evaluated as a measure of cytotoxicity and cell proliferation. The genotoxic potential of TiO₂ NPs was evaluated by scoring the number of MN in 2000 binucleated cells. The MN frequency in mononucleated cells was also considered in order to distinguish between aneuploidogenic and clastogenic effects (16). Finally, nucleoplasmic bridges (NPB), a biomarker of DNA misrepair and/or telomere end-fusions, and nuclear buds (NBUD), a biomarker of elimination of amplified DNA and/or DNA repair complexes, were also scored per 2000 binucleated cells.

MN flow cytometric assay

Micronuclei and hypodiploid nuclei induction, cytotoxicity, cell cycle modulation and an estimation of particle uptake were evaluated by flow cytometry. BEAS-2B cells were seeded in 96-well plates and exposed to NM100, NM101 or NM103 TiO₂ dispersions at 1, 5, 15 or 30 µg/ml (0.07–3.9 µg/cm²) for 48 h. Mitomycin-C at 0.05 µg/ml was used as a positive control. In Vitro Microflow Kit (Litron Laboratories) was used following manufacturer's instructions. Briefly, after exposures the cells were washed twice with phosphate-buffered saline and incubated with ethidium monoazide stain (EMA) on ice for 30 min under cold white light to allow stain photoactivation. Subsequently, cells were lysed and stained with SYTOX green for 1.5 h in the dark at 37°C. BD Accuri C6 flow cytometer with flow set to 30 µl/min and run limit of the samples set to 5000 gated nuclei events per sample was used to analyse samples. Analysis of the plots and gating of healthy nuclei, MN, apoptotic/necrotic nuclei, hypodiploid nuclei and nuclei-to-bead ratio were performed according to the manufacturer's instructions using the BD Accuri C6 software. The side-scattered light was used as an estimate of NPs uptake by comparing the mean side-scattered light area, excluding both beads and gated apoptotic/necrotic events, between controls and exposed samples (see [Supplementary Figure S1](#), available at [Mutagenesis Online](#)).

Mini-gel comet assay

DNA strand breaks and additional DNA strand breaks caused by light were assessed using alkaline comet assay. Fpg enzyme (kindly provided by Prof. Andrew Collins, University of Oslo, Oslo, Norway) mainly detects purine oxidation products, and therefore was used to evaluate oxidative DNA damage (Fpg sites). A mini-gel version of alkaline comet assay was used. BEAS-2B cells were seeded in 48 well plates and exposed to NM100, NM101 or NM103 TiO₂ dispersions at 1, 5 or 15 µg/ml (0.2–3.15 µg/cm²) for 3 or 24 h. About 2 µM Ro 19-8022 photosensitiser (Hoffman-La Roche) together with light irradiation was used as a positive control. Cells were detached from the plates using trypsin and for each sample, 30 µl of cell suspension (1.5 × 10⁴ cells) was mixed with 300 µl of 1% low-melting point agarose (Sigma–Aldrich) at 37°C. Next, 20 µl aliquots were added as drops onto eight different microscope slides pre-coated with 0.5% normal-melting point agarose (Sigma–Aldrich) and eight mini-gels were made on each slide as schematised in [Figure 1](#). Gels were left at 4°C for 5 min, and cells were lysed with a freshly prepared 1% Triton X-100 lysis buffer (2.5 M NaCl, 0.1 M EDTA, 10 mM Tris, pH 10) for 1 h in dark on ice.

After lysis, four of each set of eight slides were covered twice with 200 µL of Fpg-reaction buffer (40 mM HEPES, 0.1 M KCl, 0.5 mM EDTA, 0.2 mg/ml BSA, pH 8.0). Then, 25 µL of Fpg-reaction buffer was added on two slides (Fpg buffer), whereas the others two slides (Fpg) received 25 µl of Fpg enzyme diluted 1:3000 in Fpg-reaction buffer. All the four slides were then incubated in a humidity chamber at 37°C for 30 min. Five minutes before alkaline treatment, two of the four slides remaining in the lysis buffer were exposed to normal lab light from a OSRAM L 58W fluorescent tube ~120 cm over the lab bench giving rise to 65 µW/cm² ultraviolet (UV) light for 3 min (photoactivation). Unwinding of the DNA was then performed for all slides together in alkaline solution (0.3 M NaOH, 1 mM EDTA) for 40 min, on ice in darkness, followed by electrophoresis for 30 min (29 V, 1.15 V/cm). Before electrophoresis, the two 'photoactivation' slides were exposed again for 3 min to 65 µW/cm² UV light. All the slides were neutralised 2 × 5 min in 0.4 M Tris, dipped in deionised water and left to dry overnight. Fixation was performed in methanol for 5 min. DNA was stained by immersing air-dried slides in 1:10 000 SYBR-green diluted in 1 × TAE buffer (Sigma–Aldrich) for 30 min. A fluorescence microscope (Leica DMLB) with comet assay IV software (Perceptive Instruments) was used to score at least 50 cells per sample, and the results were expressed as mean % DNA in tail. The level of Fpg sites was calculated by subtracting the value of % DNA in the tail obtained without added enzyme from the value when the enzyme was present.

Statistical analysis

Statistical analysis was performed using GraphPad Prism 5 statistical software (GraphPad Inc.). One-way analysis of variance followed by Bonferroni's multiple comparison test ($P < 0.05$) was used to test for significance between exposures, while correlation analyses were performed by Pearson correlation (two tailed, $P < 0.05$). Results are expressed as means ± standard error of means (SEM, $n = 3$), if not differently indicated.

Results

Particle size in cell media by DLS

The TiO₂ NM tested in this study are JRC reference materials that have been well characterised previously (12). To complement this characterisation, DLS method was used to analyse particle size in

the cell media (BEGM with supplements) immediately after preparation (0h) and after 24h in 37°C. As shown in Table 1, the DLS analyses showed in general agglomerate sizes around 300–500 nm for the anatase TiO₂ (NM100 and NM101) and around 230 nm for the rutile (NM103). No large time-dependent differences in size were observed. The polydispersity index of the samples was ranging ~0.2–0.5 indicating that TiO₂ NPs were relatively non-homogeneously dispersed in cell culture medium. As shown in Supplementary Figure S1, available at *Mutagenesis* Online, the mean average size of particle agglomerates appears to dramatically change in the presence of cells.

Flow cytometric analysis of particle uptake

A clear increase in side scatter of the nuclei from TiO₂ NP-exposed cells was observed (see Figure S1), suggesting that this shift could be used to indicate cellular uptake. The mean distribution of side-scattered light increased in a linear-dependent fashion with increasing mass concentrations of all tested particles, indicating that all particles were taken up by the BEAS-2B cells (Figure 2). Both anatase TiO₂ NPs increased the side scatter to a higher extent compared to the rutile, suggesting a somewhat higher uptake of the NM100 and NM101.

Cytotoxic effects

Various methods were used to assess cytotoxic effects following TiO₂ NP exposure. The results show in general no or low effects at

the doses tested. As evaluated by Alamar blue assay, only NM103 caused a slight decrease in viability at the doses from 36 µg/ml after 3-h exposure (Figure 3a). No significant signs of cytotoxicity were seen after 48-h exposures (Figure 3b). In order to get further information of cytotoxicity, data from the MN assay were used. The cyto version of MN assay allows to simultaneously detect cytostasis and cytotoxicity in terms of cell proliferation, the percentage of cells undergoing mitosis, and apoptosis/necrosis induction. The proportion of completed cell division in TiO₂-exposed cultures was not different from unexposed cultures (Figure 3c), and no significant changes in mitotic index were observed (Figure 3d). However, a slight increase in apoptosis/necrosis was observed by microscopy for all particles at 15 µg/ml (Figure 4a). These results were also observed using flow cytometry for NM101 and NM103, but not for NM100 (Figure 4b). The agreement between the two methods was also supported by a significant correlation ($r = +0.92$, $P < 0.0001$) between the obtained results (Figure 4c). Flow cytometer analysis of cell cycle perturbations showed no significant effects of the TiO₂ exposure except from a slight decrease of G1 cells for one concentration of the NM100 (Figure 4d). The flow-based relative cells survival measurement in terms of nuclei-to-bead ratio showed no significant influence on cell proliferation following BEAS-2B exposure to TiO₂ (Supplementary Figure S3). No substantial interferences between free NPs and flow cytometry measurements were indicated (see also Supplementary Figures S1 and S2, available at *Mutagenesis* Online).

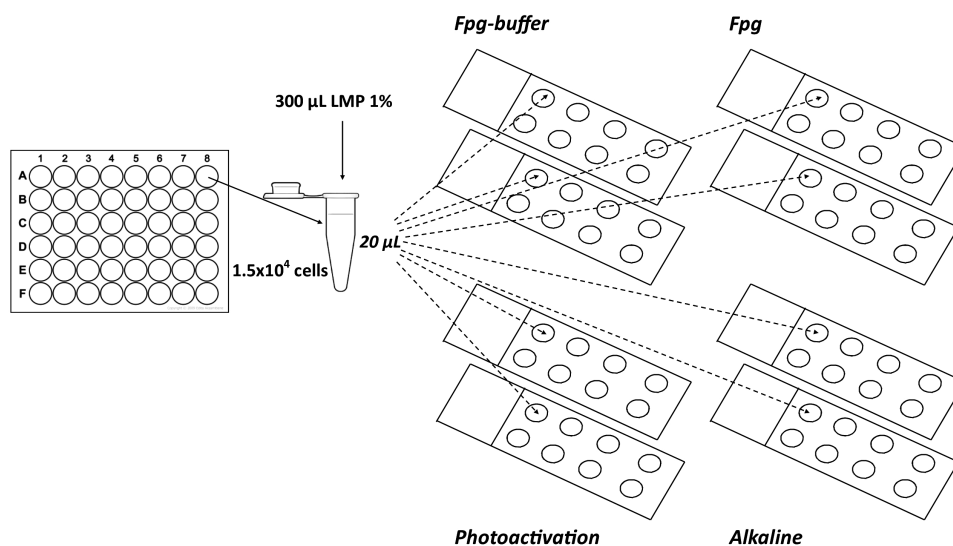


Figure 1. Schematic representation of mini-gel version of comet assay to simultaneously evaluate DNA strand breaks, oxidative DNA damage and additional DNA strand breaks induced by light.

Table 1. Polydispersity index (Pdl), zeta potential (ZP) and average size (Z-Ave) of 1 or 15 µg/ml NM100, NM101 and NM103 in the exposure medium (0 and 24 h)

Sample (µg/ml)	Medium (0h)			Medium (24 h)		
	Pdl	ZP (mV)	Z-Ave (d.nm)	Pdl	ZP (mV)	Z-Ave (d.nm)
NM100 1	0.42 ± 0.03	-9.7 ± 1.4	369 ± 45	0.42 ± 0.04	-9.1 ± 1.2	340 ± 31
NM100 15	0.22 ± 0.01	-10.3 ± 1.7	347 ± 13	0.49 ± 0.04	-18.8 ± 1.6	466 ± 56
NM101 1	0.55 ± 0.07	-8.3 ± 0.9	344 ± 68	0.43 ± 0.06	-9.1 ± 0.8	307 ± 63
NM101 15	0.40 ± 0.04	-9.5 ± 1.0	531 ± 42	0.46 ± 0.03	-9.7 ± 0.9	430 ± 47
NM103 1	0.32 ± 0.02	-9.5 ± 1.2	222 ± 12	0.27 ± 0.04	-8.8 ± 0.8	213 ± 7
NM103 15	0.26 ± 0.04	-9.2 ± 0.9	238 ± 19	0.18 ± 0.03	-9.1 ± 0.9	224 ± 6

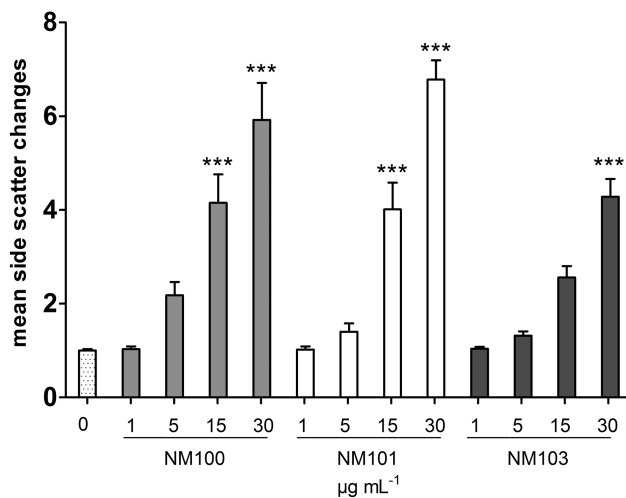


Figure 2. Estimation of BEAS-2B cellular uptake after 48-h exposure to TiO₂ NM100, NM101 and NM103, assessed by monitoring the side scatter shift in flow cytometry experiments. The results are presented as fold induction respective to the untreated control. ****P* < 0.001.

DNA strand breaks and oxidation

Mini-gel alkaline comet assay was used to detect DNA strand breaks and Fpg-sensitive sites in BEAS-2B cells following 3- or 24-h exposure to NM100, NM101 or NM103 (Figure 5). No induction of DNA strand breaks was observed following 3-h exposure, whereas 24-h exposure caused a slight but non-significant increase of DNA strand breaks. In contrast, all particles increased DNA oxidation for one or two of the concentrations following 3 h (NM100 and NM103) or 24 h (NM101).

Additional DNA strand breaks caused by light

To test if photocatalytic properties of NPs can increase DNA damage during the comet assay procedures, separate slides were exposed to normal lab light for 3 min after both the lysis and DNA unwinding steps. All tested concentrations of NM100 and the highest of NM101 significantly increased DNA damage compared to the untreated control exposed to light (Figure 6a). In terms of fold changes compared to the normal dark conditions (Figure 5, DNA damage 24h), both anatase forms of TiO₂ (NM100 and NM101) increased DNA damage in a dose-dependent manner with the NM100 being more

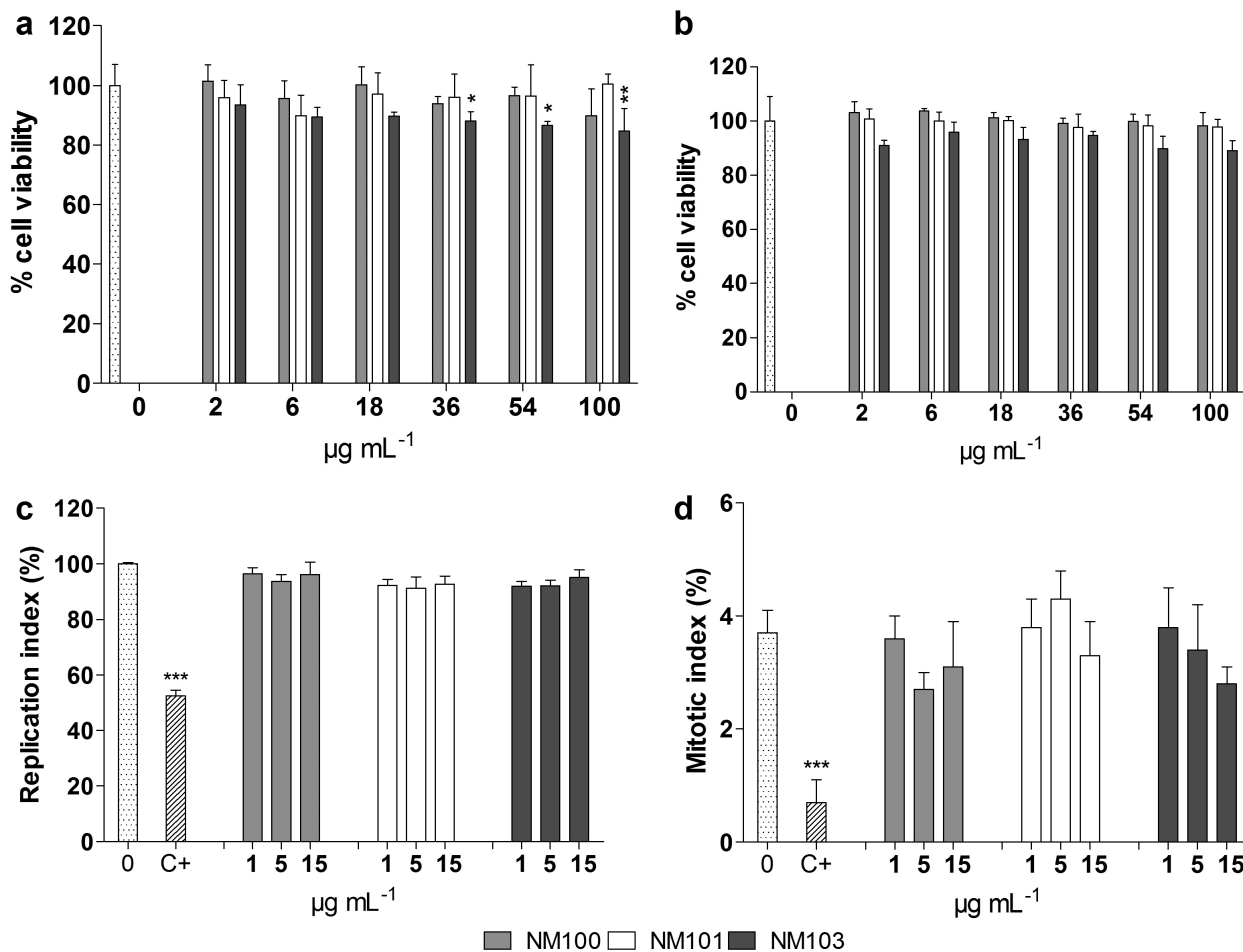


Figure 3. Cell viability of BEAS-2B cells after (a) 3-h or (b) 48-h exposure to TiO₂ NM100, NM101 or NM103 (2–100 µg/ml) assessed using Alamar Blue assay. Nuclear replication index (c) and mitotic index (d) of BEAS-2B were measured by CBMN Cyt assay following 48-h exposure to particles. C+, 0.05 µg/ml mitomycin-C. **P* < 0.05, ****P* < 0.001.

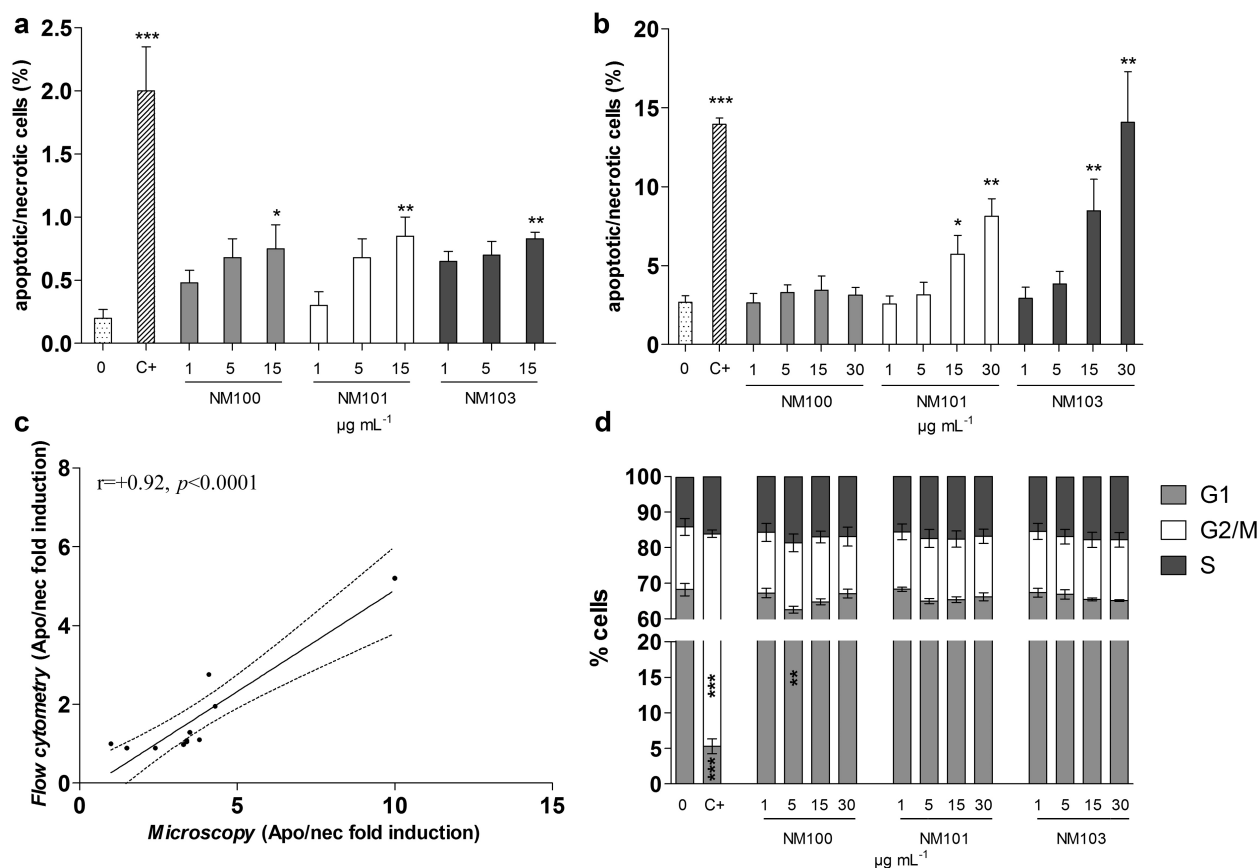


Figure 4. Induction of apoptotic and necrotic cells analysed by microscopy (a) and flow cytometry (b) following 48-h BEAS-2B exposure to particles. (c) Pearson correlation between the microscopy and the flow cytometer evaluation methods. (d) Cell cycle analysis of BEAS-2B using flow cytometry following 48-h exposure to particles. C+, 0.05 μg/ml, mitomycin-C. * $P < 0.05$, ** $P < 0.01$, *** $P < 0.001$.

effective. No significant additional DNA damage was observed after rutile TiO₂ exposure (NM103) (Figure 6b).

Chromosomal damage

MN induction was analysed both by microscopy using cytochalasin-B in a delayed co-treatment to blocking the cytokinesis (Figure 7a), and by flow cytometry without using cytochalasin-B (Figure 7b). Both methods consistently identified an increase in MN induced by the rutile NM103 in the lowest concentrations tested (1 and 5 μg/ml). The other particles were negative except the lowest concentration of NM101, which induced significant MN levels when evaluated by flow cytometry (Figure 7b). A significant statistical correlation ($r = +0.85$, $P = 0.0021$) was found between microscopy and flow cytometry results indicating that the delayed co-treatment with cytochalasin-B did not interfere with the outcome of MN assay (Figure 7c). Hypodiploid nuclei were evaluated as a measure of aneugenicity potential of TiO₂ NPs indicating no significant increase respect to the control. However, when the percentage of MN was significantly different from the control (NM101 and NM103), a slight increase of hypodiploid nuclei was noticed (Figure 7d). Coherently, MN in mononucleated cells (by microscopy) was also evaluated as a measure of aneuploidogenic potential of TiO₂ NPs, and no statistically significant differences compared to the untreated controls were observed (data not shown).

Chromosome rearrangements

NPB and NBUD were simultaneously evaluated in the CBMN Cyt assay as markers of chromosomal instability mainly due to misrepair

of DNA breaks and the process of elimination of amplified DNA (or DNA repair complexes), respectively. A slight increase of these nuclear anomalies was found and was significant for NPB following exposure to NM100 at 5 μg/ml (Figure 8).

Discussion

In this study, we explored the use of more efficient approaches to analyse the cytotoxic and genotoxic potential of TiO₂ NPs. Three reference materials varying in primary size and crystalline phase were investigated following exposure of human bronchial epithelial BEAS-2B cells able to grow in serum-free media. Harmonised operating procedures were used to disperse NPs due to experimental and regulatory needs for consistent testing strategies allowing a better understanding of toxicological outcomes associated to NPs characteristics (17).

Mini-gel comet assay and 96-well microplate-based flow cytometric analysis of micronuclei resulted in reliable and time-saving procedures giving extensive information on cytostatic, cytotoxic and genotoxic potential of TiO₂ NPs. The mini-gel version of the comet assay provided the opportunity to test for DNA strand breaks, oxidative DNA damage as well as photogenotoxicity for all three TiO₂ NPs at different mass concentrations with concurrent negative and positive controls in a single experiment. Furthermore, the flow cytometer-based analysis allowed for a faster analysis of MN, and it showed a significant correlation with the conventional microscopic-based approach. In addition, the flow cytometer based analysis gave

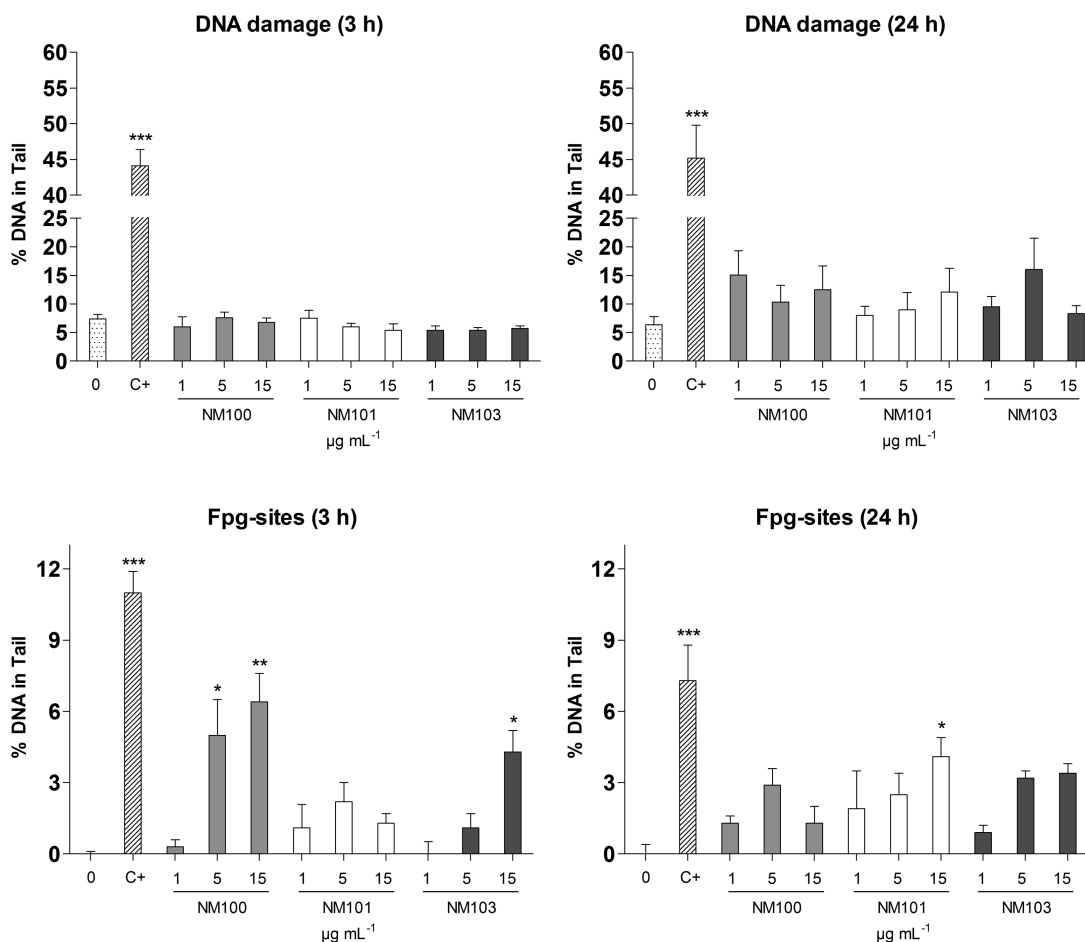


Figure 5. DNA strand breaks and Fpg-sensitive sites in BEAS-2B cells after 3- or 24-h exposure to TiO₂ NM100, NM101 or NM103 (1, 5 or 15 µg/ml) assessed using mini-gel alkaline comet assay and Fpg-modified version, respectively. **P* < 0.05, ***P* < 0.01, ****P* < 0.001. C+, 2 µM Ro together with light irradiation.

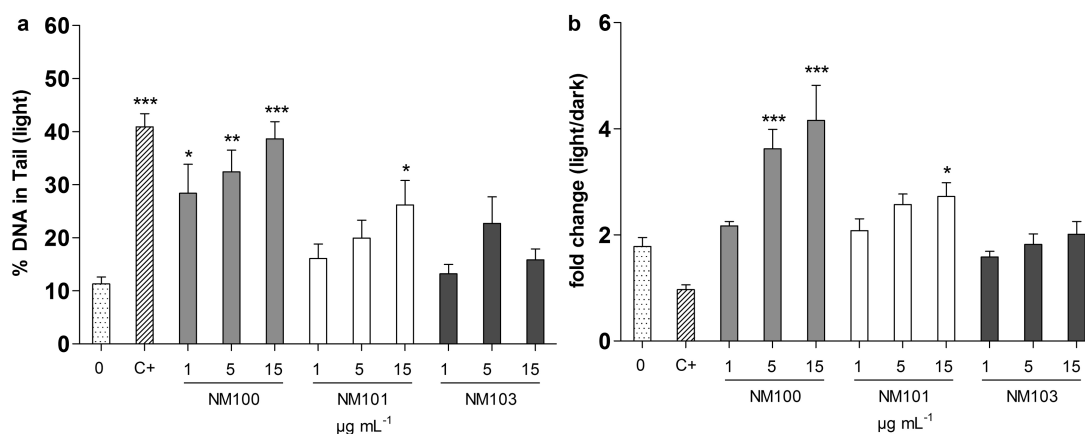


Figure 6. Additional DNA strand breaks caused by light. BEAS-2B cells were exposed to particles for 24 h, and comet slides were exposed to normal lab light for 3 min + 3 min (after lysis and alkaline treatment, respectively). Results are presented as mean ± SEM (a) and fold change compared to dark conditions (as shown in Figure 5) (b). **P* < 0.05, ***P* < 0.01, ****P* < 0.001. C+, 2 µM Ro together with light irradiation.

the opportunity to analyse higher doses, which was hard to score by the microscopic-based approach due to the difficulties in distinguishing fluorescent particle agglomerates from micronuclei. Similarly, Vallabani *et al.* (18) recently suggested that following HepG2 exposures to high TiO₂ mass concentrations, the flow cytometry approach was more reliable compared to the microscopy-based conventional method due to the accumulation of particles on prepared slides

hindering a correct evaluation of micronuclei. Except from higher throughput and more objective scoring, the flow cytometry version provide benefits due to the fact that it gives extensive information on cytotoxic effects since relative survival values can be obtained (by using nuclei-to-bead measurements) as well as information on necrosis/apoptosis (%EMA positive events) and perturbations to the cell cycle (SYTOX fluorescence distribution of nuclei) (19). Furthermore,

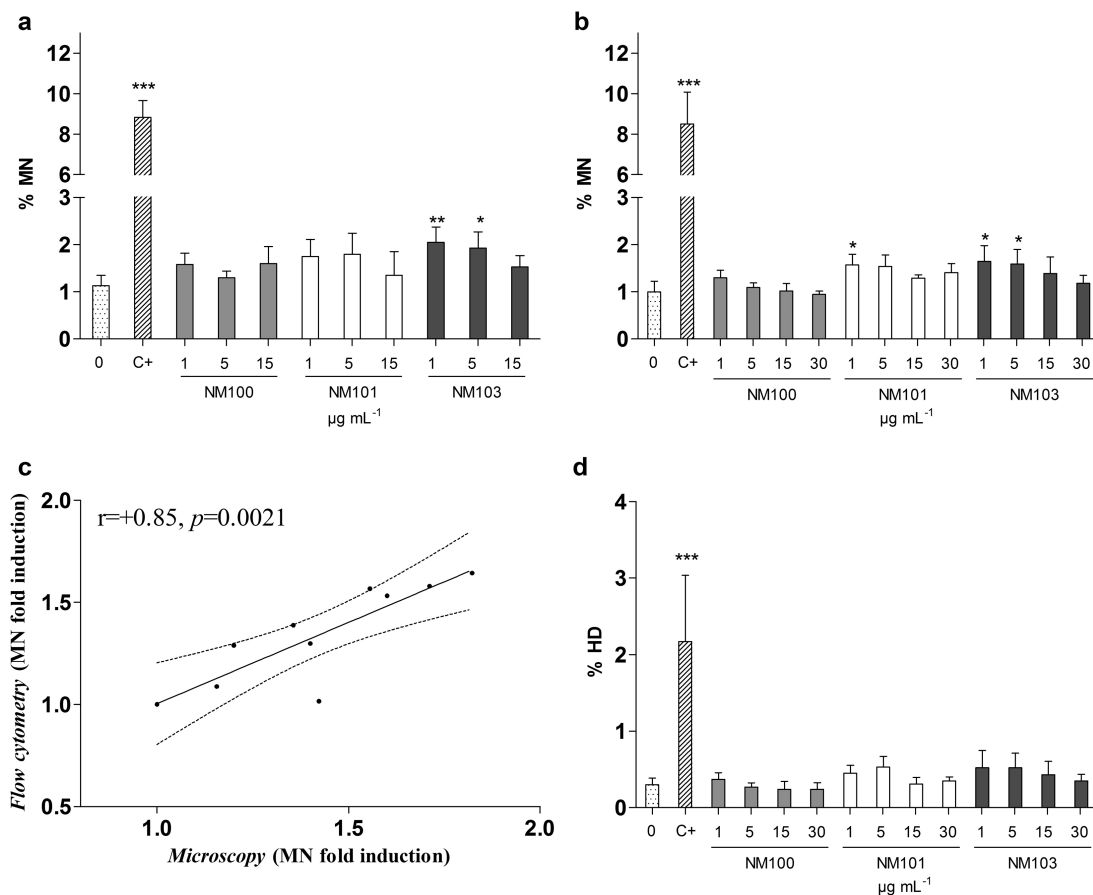


Figure 7. Micronuclei induction analysed by microscopy (a) and by flow cytometry (b) following 48-h BEAS-2B exposure to particles. (c) Pearson correlation between MN induction assessed by flow cytometry and microscopy. (d) Percentage of hypodiploid nuclei (HD). * $P < 0.05$, ** $P < 0.01$, *** $P < 0.001$. C+, 0.05 $\mu\text{g/ml}$ mitomycin-C.

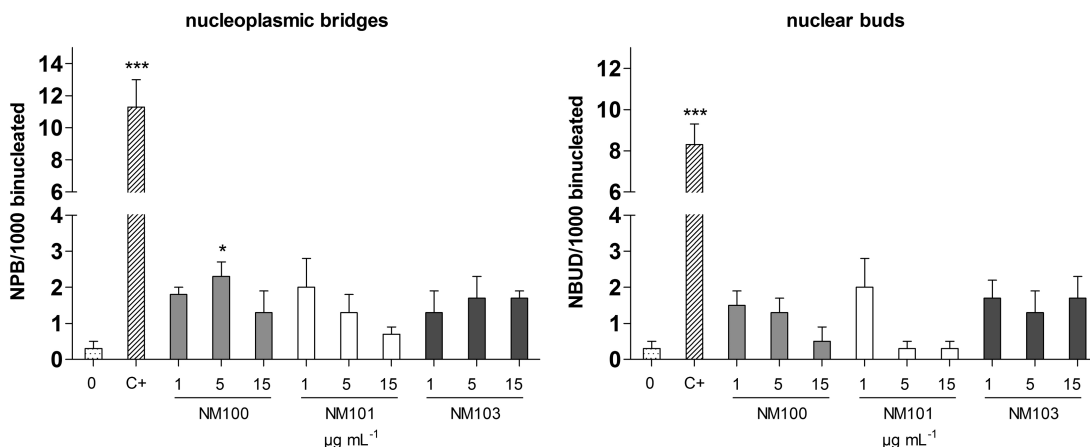


Figure 8. Chromosome rearrangements in terms of nucleoplasmic bridges and nuclear buds analysed by microscopy (CBMN Cyt assay) following 48-h BEAS-2B exposure to particles. * $P < 0.05$, ** $P < 0.01$, *** $P < 0.001$. C+, 0.05 $\mu\text{g/ml}$ mitomycin-C.

by analysing the increase of the frequency of hypodiploid nuclei, the flow cytometer approach is sensitive not only to clastogens but also to aneuploidogens that interfere with the migration of chromosomes to spindle poles (20). This is important to analyse in a high-throughput manner since NM seem to exert their genotoxic potential also by mechanically interfering with the microtubules (21). Interestingly, recent studies on HepG2 cells exposed to silver nanoparticles (20

and 50 nm) show not only an increase in MN frequency but also a dose-dependent increase in hypodiploid cells, thus suggesting involvement of aneugenicity (22,23).

We found no or low effects on cytotoxicity at the doses tested despite clear increase in side scatter suggesting a pronounced particle uptake. The most sensitive assay appeared to be the flow cytometer analysis of necrotic/apoptotic cells showing a clear and

dose-dependent increase for NM101 and NM103. The cytotoxicity of TiO₂ NPs in cultured lung cells has shown different outcomes in different studies. For instance, large agglomerates of rutile and anatase TiO₂ were reported to be internalised in A549 human alveolar epithelial cells and to cause an induction of intracellular reactive oxygen species (ROS) generation and a reduction in cell viability (only the anatase), but only at high doses (>250 µg/ml) (24). Furthermore, in BEAS-2B cells, TiO₂ NPs (P-25 Degussa) were observed in the cytoplasm shortly after exposure and around the perinuclear region following longer exposures, and markers for oxidative stress, inflammation and apoptosis were increased at the doses tested (up to 40 µg/ml) (25). Conversely, in a recent study, similar concentrations of TiO₂ P-25 NPs were not cytotoxic toward BEAS-2B cells, but altered several canonical signalling pathways including cell cycle regulation, apoptosis, calcium signalling, NRF2-mediated oxidative response, cell adhesion and inflammatory response among others (26). The inconsistent cytotoxicity of TiO₂ P-25 NPs could be due to the different cell culture conditions used in these studies where BEAS-2B cells were grown in the presence of 10% fetal bovine serum in the former and in a serum-free condition in the latter. The importance of TiO₂ crystalline phase was highlighted in a recent study in which bulk and NP rutile TiO₂ showed greater cytotoxicity compared to bulk and NP anatase in terms of impairment of Balb/3T3 mouse fibroblasts clonogenicity, and the effects were not explained by differences in uptake (27).

The Janus-faced characteristic of TiO₂ NPs being able to absorb and scatter UV radiation represents an additional toxicological hazard due to photoactivation. For instance, it was shown that TiO₂ NPs were inert up to 100 µg/ml following exposure of murine RAW264.7 macrophages, while after photoactivation the cytotoxicity was significantly increased and depended on the surface area of the particles as well as their hydroxyl radical generation ability (28). Furthermore, anatase TiO₂ NPs showed higher photocytotoxicity compared to rutile TiO₂ NPs in various cell types (29–31), although radical generation has also been reported in dark conditions (32). Serum proteins bound to the TiO₂ nanostructures could, however, scavenge photogenerated radicals, and thus prevent phototoxic effects (33). Although several physico-chemical characteristics play a role in NPs-induced genotoxicity, ROS generation ability is widely considered among the most relevant, thus highlighting the importance of polymorph TiO₂ surface reactivity for their genotoxic potentials (34).

When using the mini-gel comet assay our study showed no increase in DNA strand breaks but a clear induction of Fpg sites, particularly following 3-h exposure to NM100 (Figure 7). The Fpg enzyme detects oxidised purines, mainly 8-oxoguanine, as well as formamidopyrimidines (such as fapy-guanine) and is the most widely used enzyme in nanotoxicology research. It should, however, be noted that it has been reported to also detect alkylation damage, and alternatives such as hOGG1 (human 8-hydroxyguanine DNA-glycosylase 1) could offer a more specific alternative (35). The question has been raised whether NPs attached to the nucleoid in the comet assay could interfere with the enzyme possibly leading to lower detected damage (3). Such interactions have, however, only been observed in a study in which the NPs were mixed with the FPG prior to the analysis of its ability to detect Fpg sites (6), and the significance of this results for a 'real' interaction is presently not fully elucidated. Furthermore, due to the photocatalytic activity of NM100 used in this study, the possibility of artificially formed oxidised purines during assay performance cannot be totally ruled out, although it seems unlikely due to the fact that the assay was

performed in dark. Our results clearly showed that light exposure induced additional DNA strand breaks in anatase TiO₂-exposed cells, with the NM100 being more effective than NM101, while rutile TiO₂ NPs showed no activity. This is thus in line with other studies (36) as well as with our previous study showing robust light-induced DNA damage for anatase TiO₂ material but not for the rutile NM103 (3). The reason for the higher activity of the NM100 is most likely due to the fact that this material is non-coated as compared to the NM101 (12). In terms of chromosomal damage assessed by MN induction, rutile TiO₂ NPs were slightly more effective than the two anatase NPs, shown using both conventional microscopy analysis or by flow cytometry, and the response was most clear in the lower doses (1 and 5 µg/ml). Although only low levels were induced, we found a strong correlation between microscopy and flow cytometry results indicating that the delayed co-treatment with cytochalasin-B used in the conventional studies by microscopy did not interfere with the MN induction (since it was not used in flow cytometry experiments). Overall, a weak DNA damaging potential of TiO₂ NPs were observed, and the crystalline phase was mainly a critical factor for the light-induced DNA damage with anatase being most potent whereas the rutile form was slightly more effective in inducing chromosomal damage. In our recent study (3), we reviewed all *in vitro* NP studies with data from both comet assay and MN assay. We found that 19 of 22 studies reported positive results on DNA strand breakage (comet assay), while only 7 studies reported positive MN results. Thus, it appeared as the correlation between the assays was rather poor for TiO₂ (in contrast to other NPs). In the present study, however, there was a good consistency between DNA strand breaks and MN formation for NM100 and NM101 showing negative results. In contrast the rutile NM103 did not cause DNA strand breaks but a slight increase in MN formation. The weak genotoxic effects were observed already at 1 µg/ml (0.2 µg/cm²), and this can be related to human exposures considering e.g. a worker exposed to 0.3 mg/m³ (NIOSH limit value for ultrafine TiO₂). With the same assumptions as in Wang *et al.* (37) and considering that the deposition can be 10 times higher at certain locations ('hot spots') in the lung, this cell dose can be obtained following ~1-month occupational work.

TiO₂ NPs and fine rutile particles have previously been reported to induce DNA damage in BEAS-2B cells exposed in serum-free conditions, although only anatase TiO₂ NPs were able to slightly induce MN after 72-h treatment (8). Furthermore, in serum-containing BEAS-2B cultures, a slightly higher level of oxidative DNA damage was induced following a short exposure to a mix of anatase-rutile NPs compared to exposures with either anatase or rutile particles alone (38). Indeed, DNA damage at a certain time is the result of continuous DNA damage generation and repair processes. Thus, the difference in sensitivity between the comet assay and MN test, often performed at different time points, could partly be the result of different impact on cellular DNA repair ability. TiO₂ NPs have been shown to significantly impair DNA repair activity, both the base and nucleotide excision repair pathways, in A549 cells in addition to inducing oxidative stress and genotoxicity (39).

Conclusion

In this study, weak genotoxic effects of the tested TiO₂ materials was found with an induction of oxidative DNA damage for all three materials and a slight increase in MN formation for NM103. A clear induction of DNA strand breaks was observed for the anatase materials when the comet slides were briefly exposed to normal lab light. This highlights the risk of false positives when testing

photocatalytically active materials if light is not properly avoided. We conclude that mini-gel comet assay and MN scoring using flow cytometry successfully can be used to efficiently study cytotoxic and genotoxic properties of NPs.

Supplementary data

Supplementary Figures 1–3 are available at *Mutagenesis* Online.

Funding

This study was supported by the Swedish Research Council (VR, project 621-2014-4598); Swedish Research Council for Health, Working Life and Welfare (FORTE, project 2011-0832); the European Union Seventh Framework Programme (FP7/2007-2013) under the project NANoREG, a common European approach to the regulatory testing of nanomaterials (grant number 310584); and the Cancer and Allergy Foundation (Sweden).

References

- Harris, G., Palosaari, T., Magdolenova, Z., Mennecozzi, M., Gineste, J. M., Saavedra, L., Milcamps, A., Huk, A., Collins, A. R., Dusinska, M. and Whelan, M. (2015) Iron oxide nanoparticle toxicity testing using high-throughput analysis and high-content imaging. *Nanotoxicology*, 1, 87–94.
- Gonzalez, L., Sanderson, B. J. and Kirsch-Volders, M. (2011) Adaptations of the in vitro MN assay for the genotoxicity assessment of nanomaterials. *Mutagenesis*, 26, 185–191.
- Karlsson, H. L., Di Bucchianico, S., Collins, A. R. and Dusinska, M. (2015) Can the comet assay be used reliably to detect nanoparticle-induced genotoxicity? *Environ. Mol. Mutagen.*, 56, 82–96.
- Karlsson, H. L. (2010) The comet assay in nanotoxicology research. *Anal. Bioanal. Chem.*, 398, 651–666.
- Lin, M. H., Hsu, T. S., Yang, P. M., Tsai, M. Y., Perng, T. P. and Lin, L. Y. (2009) Comparison of organic and inorganic germanium compounds in cellular radiosensitivity and preparation of germanium nanoparticles as a radiosensitizer. *Int. J. Radiat. Biol.*, 85, 214–226.
- Kain, J., Karlsson, H. L. and Möller, L. (2012) DNA damage induced by micro- and nanoparticles—interaction with FPG influences the detection of DNA oxidation in the comet assay. *Mutagenesis*, 27, 491–500.
- Magdolenova, Z., Lorenzo, Y., Collins, A. and Dusinska, M. (2012) Can standard genotoxicity tests be applied to nanoparticles? *J. Toxicol. Environ. Health A*, 75, 800–806.
- Falck, G. C., Lindberg, H. K., Suhonen, S., Vippola, M., Vanhala, E., Catalán, J., Savolainen, K. and Norppa, H. (2009) Genotoxic effects of nanosized and fine TiO₂. *Hum. Exp. Toxicol.*, 28, 339–352.
- Shi, H., Magaye, R., Castranova, V. and Zhao, J. (2013) Titanium dioxide nanoparticles: a review of current toxicological data. *Part. Fibre Toxicol.*, 10, 15.
- Prasad, R. Y., Wallace, K., Daniel, K. M., Tennant, A. H., Zucker, R. M., Strickland, J., Dreher, K., Kligerman, A. D., Blackman, C. F. and Demarini, D. M. (2013) Effect of treatment media on the agglomeration of titanium dioxide nanoparticles: impact on genotoxicity, cellular interaction, and cell cycle. *ACS Nano*, 7, 1929–1942.
- Magdolenova, Z., Bilaničová, D., Pojana, G., Fjellsbø, L. M., Hudcová, A., Hasplová, K., Marcomini, A. and Dusinska, M. (2012) Impact of agglomeration and different dispersions of titanium dioxide nanoparticles on the human related in vitro cytotoxicity and genotoxicity. *J. Environ. Monit.*, 14, 455–464.
- Rasmussen, K., Mast, J., De Temmerman, P.-J. et al. (2014) Titanium dioxide, NM-100, NM-101, NM-102, NM-103, NM-104, NM-105: characterization and physico-chemical properties, EUR—Scientific and Technical Research Series. Publications Office of the European Union, Luxembourg.
- Fenech, M. (2007) Cytokinesis-block micronucleus cytochrome assay. *Nat. Protoc.*, 2, 1084–1104.
- Di Bucchianico, S., Fabbrizi, M. R., Cirillo, S., Ubaldi, C., Gilliland, D., Valsami-Jones, E. and Migliore, L. (2014) Aneuploidogenic effects and DNA oxidation induced in vitro by differently sized gold nanoparticles. *Int. J. Nanomedicine*, 9, 2191–2204.
- OECD. (2014) *Guidelines for the Testing of Chemicals, In Vitro Cell Micronucleus Test, Test No. 487. Section 4: Health Effects*. OECD Publishing, Paris.
- Rosefort, C., Fauth, E. and Zankl, H. (2004) Micronuclei induced by aneugens and clastogens in mononucleate and binucleate cells using the cytokinesis block assay. *Mutagenesis*, 19, 277–284.
- Hartmann, N. B., Jensen, K. A., Baun, A. et al. (2015) Techniques and protocols for dispersing nanoparticle powders in aqueous media—is there a rationale for harmonization? *J. Toxicol. Environ. Health. B. Crit. Rev.*, 18, 299–326.
- Vallabani, N. V. S., Shukla, R. K., Konka, D., Kumar, A., Singh, S. and Dhawan, A. (2014) TiO₂ nanoparticles induced micronucleus formation in human liver (HepG2) cells: comparison of conventional and flow cytometry based methods. *Mol. Cytogenet.*, 7 (Suppl. 1), P79.
- Avlasevich, S., Bryce, S., De Boeck, M., Elhajouji, A., Van Goethem, F., Lynch, A., Nicolette, J., Shi, J. and Dertinger, S. (2011) Flow cytometric analysis of micronuclei in mammalian cell cultures: past, present and future. *Mutagenesis*, 26, 147–152.
- Bryce, S. M., Bemis, J. C., Avlasevich, S. L. and Dertinger, S. D. (2007) In vitro micronucleus assay scored by flow cytometry provides a comprehensive evaluation of cytogenetic damage and cytotoxicity. *Mutat. Res.*, 630, 78–91.
- Gonzalez, L., Lukamowicz-Rajska, M., Thomassen, L. C., Kirschhock, C. E., Leyns, L., Lison, D., Martens, J. A., Elhajouji, A. and Kirsch-Volders, M. (2014) Co-assessment of cell cycle and micronucleus frequencies demonstrates the influence of serum on the in vitro genotoxic response to amorphous monodisperse silica nanoparticles of varying sizes. *Nanotoxicology*, 8, 876–884.
- Sahu, S. C., Njoroge, J., Bryce, S. M., Yourick, J. J. and Sprando, R. L. (2014) Comparative genotoxicity of nanosilver in human liver HepG2 and colon Caco2 cells evaluated by a flow cytometric in vitro micronucleus assay. *J. Appl. Toxicol.*, 34, 1226–1234.
- Sahu, S. C., Njoroge, J., Bryce, S. M., Zheng, J. and Ihrie, J. (2016) Flow cytometric evaluation of the contribution of ionic silver to genotoxic potential of nanosilver in human liver HepG2 and colon Caco2 cells. *J. Appl. Toxicol.*, 36, 521–531.
- Aueviriyavit, S., Phummiratch, D., Kulthong, K. and Maniratanachote, R. (2012) Titanium dioxide nanoparticles-mediated in vitro cytotoxicity does not induce Hsp70 and Grp78 expression in human bronchial epithelial A549 cells. *Biol. Trace Elem. Res.*, 149, 123–132.
- Park, E. J., Yi, J., Chung, K. H., Ryu, D. Y., Choi, J. and Park, K. (2008) Oxidative stress and apoptosis induced by titanium dioxide nanoparticles in cultured BEAS-2B cells. *Toxicol. Lett.*, 180, 222–229.
- Thai, S. F., Wallace, K. A., Jones, C. P., Ren, H., Prasad, R. Y., Ward, W. O., Kohan, M. J. and Blackman, C. F. (2015) Signaling Pathways and Micro-RNA changes in nano-TiO₂ treated human lung epithelial (BEAS-2B) cells. *J. Nanosci. Nanotechnol.*, 15, 492–503.
- Ubaldi, C., Urbán, P., Gilliland, D., Bajak, E., Valsami-Jones, E., Ponti, J. and Rossi, F. (2016) Role of the crystalline form of titanium dioxide nanoparticles: rutile, and not anatase, induces toxic effects in Balb/3T3 mouse fibroblasts. *Toxicol. In Vitro*, 31, 137–145.
- Xiong, S., George, S., Ji, Z., Lin, S., Yu, H., Damoiseaux, R., France, B., Ng, K. W. and Loo, S. C. (2013) Size of TiO₂ nanoparticles influences their phototoxicity: an in vitro investigation. *Arch. Toxicol.*, 87, 99–109.
- Yin, J. J., Liu, J., Ehrenshaft, M., Roberts, J. E., Fu, P. P., Mason, R. P. and Zhao, B. (2012) Phototoxicity of nano titanium dioxides in HaCaT keratinocytes—generation of reactive oxygen species and cell damage. *Toxicol. Appl. Pharmacol.*, 263, 81–88.
- Sanders, K., Degn, L. L., Mundy, W. R., Zucker, R. M., Dreher, K., Zhao, B., Roberts, J. E. and Boyes, W. K. (2012) In vitro phototoxicity and hazard identification of nano-scale titanium dioxide. *Toxicol. Appl. Pharmacol.*, 258, 226–236.

31. Uchino, T., Tokunaga, H., Ando, M. and Utsumi, H. (2002) Quantitative determination of OH radical generation and its cytotoxicity induced by TiO₂-UVA treatment. *Toxicol. In Vitro*, 16, 629–635.
32. Fenoglio, I., Greco, G., Livraghi, S. and Fubini, B. (2009) Non-UV-induced radical reactions at the surface of TiO₂ nanoparticles that may trigger toxic responses. *Chemistry*, 15, 4614–4621.
33. Garvas, M., Testen, A., Umek, P., Gloter, A., Koklic, T. and Strancar, J. (2015) Protein corona prevents TiO₂ phototoxicity. *PLoS One*, 10, e0129577.
34. Fubini, B., Ghiazza, M. and Fenoglio, I. (2010) Physico-chemical features of engineered nanoparticles relevant to their toxicity. *Nanotoxicology*, 4, 347–363.
35. Smith, C. C., O'Donovan, M. R. and Martin, E. A. (2006) hOGG1 recognizes oxidative damage using the comet assay with greater specificity than FPG or ENDOIII. *Mutagenesis*, 21, 185–190.
36. Møller, P., Hemmingsen, J. G., Jensen, D. M. *et al.* (2015) Applications of the comet assay in particle toxicology: air pollution and engineered nanomaterials exposure. *Mutagenesis*, 30, 67–83.
37. Wang, X., Ji, Z., Chang, C. H. *et al.* (2014) Use of coated silver nanoparticles to understand the relationship of particle dissolution and bioavailability to cell and lung toxicological potential. *Small*, 10, 385–398.
38. Gurr, J. R., Wang, A. S., Chen, C. H. and Jan, K. Y. (2005) Ultrafine titanium dioxide particles in the absence of photoactivation can induce oxidative damage to human bronchial epithelial cells. *Toxicology*, 213, 66–73.
39. Jugan, M. L., Barillet, S., Simon-Deckers, A., Herlin-Boime, N., Sauvaigo, S., Douki, T. and Carriere, M. (2012) Titanium dioxide nanoparticles exhibit genotoxicity and impair DNA repair activity in A549 cells. *Nanotoxicology*, 6, 501–513.